*Desalination and Water Treatment*
www.deswater.com

doi: 10.1080/19443994.2015.1112978

57 (2016) 20199–20209
September

Taylor & Francis
Taylor & Francis Group

# Finding sources and sinks of fluorescent dissolved organic matter in a riverine system using parallel factor model

Aamir Alaud Din[a], Yongeun Park[b], Seung Won Lee[c], Sung Min Cha[d], Kyung Hwa Cho[e], Joon Ha Kim[a,*]

[a]*School of Environmental Science and Engineering, Gwangju Institute of Science and Technology (GIST), 261 Cheomdan-gwagiro, Buk-gu, Gwangju 500-712, Korea, email: joonkim@gist.ac.kr (J.H. Kim)*
[b]*Environmental Microbial and Food Safety Laboratory, United States Department of Agriculture-Agricultural Research Service, 10300 Baltimore Avenue, Belstville, MD 20705, USA*
[c]*Environmental and Plant Engineering Research Institute, Korea Institute of Civil Engineering and Building Technology (KICT), 283, Goyangdae-Ro Ilsanseo-Gu, Goyang-Si, Gyeonggi-Do 10223, Korea*
[d]*Jeollanam-do Environmental Industries Promotion Institute, Gangjin-gun, Jeollanam-do 527-811, Korea*
[e]*School of Urban and Environmental Engineering, Ulsan National Institute of Science and Technology (UNIST), 100 Banyeon-ri, Eonyang-eup, Ulju-gun, Ulsan 698-805, Korea*

Received 15 August 2015; Accepted 10 October 2015

ABSTRACT

To characterize fluorescent dissolved organic matter (FDOM) in Yeongsan River in Korea, 110 water samples were acquired from March 2008 to November 2009 around the watershed. Excitation emission matrix data of fluorescence was obtained using spectrophotometric analysis and parallel factor (PARAFAC) model was used to characterize FDOM. The spatiotemporal variation and effect on FDOM were studied using an exploratory analysis and analysis of variance (ANOVA). According to the spatial and seasonal characteristics, we used *post hoc* analysis to identify significantly different sites and season. The PARAFAC results identified three most important PARAFAC components explaining 95.32% of total variance of original data-set. Seasons and sites had a significant effect on PARAFAC Components I and II ($p \leq 0.05$), whereas season had a significant effect on Component III ($p \leq 0.05$). There was no significant interaction between seasons and sites for all the three PARAFAC components ($p > 0.05$). For Components I and II, summer season was significantly different from other seasons ($p \leq 0.05$), whereas for Component III, the fall season was significantly different from winter and summer seasons ($p \leq 0.05$). These results indicate that ANOVA and *post hoc* analysis in our study not only confirmed the results of previous studies, but also revealed differences in seasons and sites for identified FDOMs as a new information. The methodology proposed in this paper can be a useful tool for finding sources and sinks of FDOMs in a riverine system influenced by natural organic matter impairment.

*Keywords:* FDOM; Yeongsan watershed (YSW); PARAFAC; Spatiotemporal analysis; ANOVA test

*Corresponding author.

## 1. Introduction

The Yeongsan River (YSR), one of the largest rivers in Korea, is a source of water for about two million people residing around the river. The YSR is also a source of water for irrigation, recreation, industrial use, and ecosystems in the South Jeolla Province [1,2]. As the primary function of the YSR is cropland irrigation [3], it has thus been the focus of studies investigating trace metal concentration profiles [1], relationships between land use type and fecal indicator bacteria and heavy metals [2], and a decline in fish diversity [3].

The major land use around the Yeongsan Watershed (YSW) is agriculture and forestation, which are the primary sources of fluorescent dissolved organic matter (FDOM). The degradation of agricultural, forest, and animal organic matter results in humus, which forms a significant fraction of the total organic matter; the two most important soluble fractions of humus are humic and fulvic acids, which are both fluorescent in nature. The dominant fractions of humus are humic acids [4,5], an ubiquitous constituent of every riverine environment, which constitutes between 40 and 60% of natural organic matter (NOM) [4]. As FDOM is light absorbing, it is also known as chromophoric-dissolved organic matter (CDOM) and can significantly influence the underwater light field. It absorbs ultraviolet light, thereby strongly restricting the penetration depth of UV-B radiation, which is harmful to living organisms [6]. Therefore, FDOM is an important area of focus for further investigation.

In recent decades, fluorescence spectroscopy has been widely used to analyze and characterize FDOM [7]. In this field, potential applications include drinking water quality monitoring [8], analysis of food products such as yogurt and fish [9,10], and studies of marine and aquatic environments [11,12].

Measurement of autofluorescence at numerous emission wavelengths for different excitation wavelengths has been carried out to obtain excitation emission matrices (EEMs). The analysis of these EEMs can be facilitated by the models such as the parallel factor analysis (PARAFAC), Tucker, and N-way partial least square regression (N-PLS) [9]. Among these models, if the data is trilinear, PARAFAC has been a powerful model for extracting information from EEM data obtained through fluorescence spectroscopy [13]. PARAFAC decomposes the fluorescent signal of the fluorophore mixture into individual fluorescent analytes and provides estimates of spectra with concentration profiles of fluorophores [9,14].

Based on our literature survey on YSW, FDOM has not been characterized in the YSW and its surrounding region, containing mainly croplands, small forests, wetlands, and urbanized areas. In this study, we concentrate on sites at which a tributary merges into the YSR and thereby contributes FDOM to the YSR. A total of 110 samples were collected over a duration of 16 months (from March 2008 to November 2009) from eight sites around the YSR (Fig. 1). The EEM data from these samples enabled us to study the spatiotemporal variability of the identified fluorophores. Compared to the other PARAFAC modeling studies of riverine and marine systems, this study is unique because we utilize the concentrations of identified chemical analytes (fluorophores) to determine major sites that contribute each identified FDOM to the YSW. We also used a simultaneous spatial and temporal bubble plot which gives more clear and additional information about FDOM fluorophores. Previous studies on FDOM characterization had been limited to spatial and temporal variation of FDOM fluorophores employing the spatial and temporal plots. In this study, we used analysis of variance (ANOVA) to determine the effect of seasons and sites on the identified FDOM fluorophores. ANOVA provided hidden information that could not be caught by simple spatial and temporal plots. We also used *post hoc* analysis to find out significantly different sites and seasons.

## 2. Materials and methods

### 2.1. Field sites description

The study area YSR, is the main stream of YSW system. Its flow length is 136 km and has an area of 3,445 $km^2$. Fig. 1 shows the eight sampling sites around the YSR where the tributaries merge with the river. The upland region consists of the Ohrye (S1) and Gwangju (S2) tributaries. The Ohrye tributary is located in an agricultural area while the Gwangju tributary is surrounded by the city of Gwangju—a highly urbanized region known as one of the largest metropolitan cities in Korea. Gwangju is also one of the most polluted areas in the YSW. The Hwangryong tributary (S3) consists of a mixed region of urbanized and agricultural areas while the Jangseong tributary (S4) is comprised of agricultural land—the largest among the eight sites. The four remaining sites, Manbong (S5), Gomakwon (S6), Sampo (S7), and Yeongam (S8) tributaries are also agricultural sites. Past the Yeongam tributary, the YSR is connected into the West Sea. The YSW system also includes four upstream dams and one estuarine dam in the basin for agricultural purposes. The eight sites mentioned comprise all of the diversity in the YSW and were thus selected as sampling sites. The samples collected from these sites

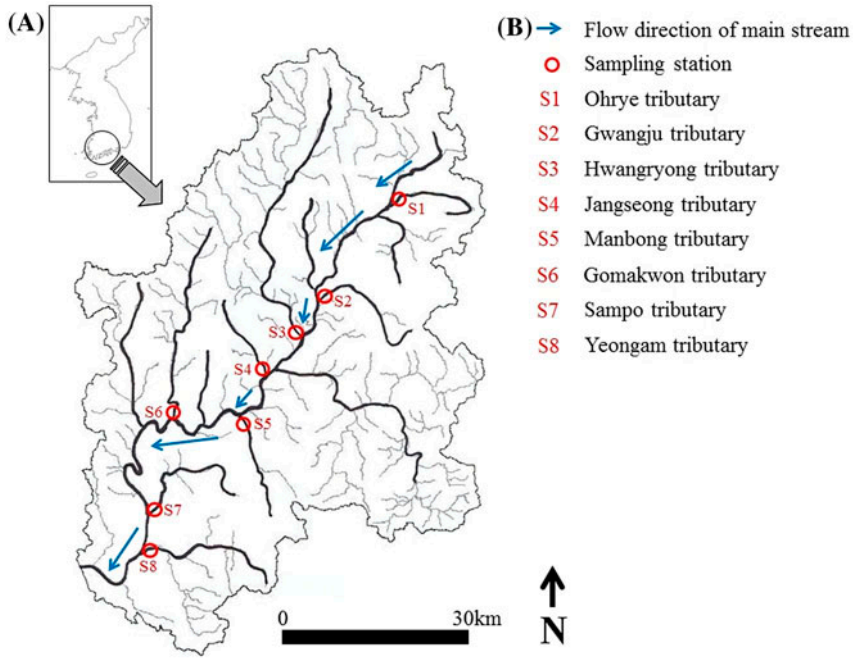


Fig. 1. (A) Map of Yeongsan Watershed (YSW) showing the eight sampling sites (red circles; from S1 to S8). Blue arrows indicate flow direction. The sampling sites are tributary end points discharging into the YSW mainstream and (B) Legends used for identifying the eight sampling stations in (A).

were analyzed to determine the sources and sinks of FDOM as well as turbidity in the YSW system [1].

### 2.2. Data acquisition

To study the spatiotemporal variation of FDOM, 110 water samples were collected from the eight sampling sites. The samples were collected in 500 mL polyethylene bottles over the 16-month period from March 2008 to November 2009. The turbidity of the water samples were analyzed *in situ* using multi-parameter water quality monitor YSI 6600 EDS (YSI Inc., USA). *In situ* measurement was performed in order to ensure data accuracy which would have otherwise been affected by the coagulation and flocculation of particles if done *ex situ*. The samples were tightly capped, stored in insulated boxes containing ice packs and were placed in the laboratory refrigerator.

Excitation emission matrix (EEM) data were then obtained through spectrophotometric analysis. For accuracy, spectrophotometric measurements were performed on the day of sampling itself to prevent photochemical decomposition of FDOM caused by prolonged storage [5]. Pre-spectrophotometric analysis steps include agitation (shaking) and filtration of the water samples through 0.45 μm pore size DISMIC®-25CS cellulose acetate filter. A 1.0 cm quartz cuvette was used to hold the sample filtrate. The cuvette was cleaned by rinsing with acetone and ethanol once and then drying, followed by rinsing thrice with triple distilled water and then drying. A computer-controlled F-2500 fluorescence spectrophotometer (HITACHI High-Technologies Corporation, Japan) was used to measure the spectra of the filtered samples. Excitation and emission wavelengths ranging from 220 nm to 600 nm in 5 nm intervals were used. The scan speed was adjusted to 1,500 nm/min with excitation and emission slits of 5 nm.

### 2.3. Fluorescence data analysis

Initial fluorescence EEM data have arbitrary units (A.U.). Pretreatment (a step required to remove instrumental biases) changes these units into quinine sulfate (Q.S.) units. This pretreatment step also allows the data to be used in PARAFAC modeling. The pretreatment of raw EEM data, PARAFAC model, and its application to the EEM data are described in detail in sections SM-1, SM-2, and SM-3 of supplementary materials, respectively.

### 2.4. Statistical analyses

Statistical analysis, ANOVA, and *post hoc* were run using statistical package for the social sciences (SPSS

17.0, SPSS Inc., USA). A $p$-value of 0.05 was used to determine the level of significance for ANOVA and *post hoc* analysis.

## 3. Results and discussion

### 3.1. Fluorescence characterization

Using the PARAFAC model, three components were found to be optimum for the EEM data (Section SM-3 in supplementary materials). To characterize the FDOM in the 110 samples, pairs of excitation emission maxima were used for all of the three PARAFAC components. The ranges of pairs of excitation emission maxima, shown in Table SM-1 (supplementary materials), are specific to different fluorophores [7,15–21]. Component-I demonstrated an excitation maximum at 355 nm and emission maximum at 450 nm. Component-II had an excitation maximum at 320 nm, with an emission maximum at 405 nm. Component-III was characterized by an excitation maximum at 280 nm with emission peak at 410 nm. These values are listed in Table 1. Component-I was identified as humic C, a humic substance found in natural waters [18]. Component-II was identified as humic C3 [19] and Component-III was found to be marine humic M [22]. Marine humic M was previously thought to have a marine source, though it can also be observed in natural water impacted by agricultural activities [22–24].

### 3.2. Spatial variation of FDOM fluorophores

To determine the spatial variation of the identified FDOM fluorophores, concentrations were plotted against each sampling month (Fig. 2). Components I and II display similar concentration profiles, indicating the possibility that the components might have originated from a common source. The concentration profile of Component III on the other hand is clearly different, showing a nearly flat trend throughout the study period except for three events (2008/04, 2009/10, and 2009/11). This suggests that Component III originated from a different source and that all sites contribute this component nearly equally.

Table 1
Identification of FDOM based on excitation emission maxima

| Component | Ex/Em (nm/nm) | Fluorophore |
|---|---|---|
| Component I | 355/450 | Humic C3 |
| Component II | 320/405 | Humic C |
| Component III | 280/410 | Marine Humic M |

From Fig. 2, it is evident that the concentrations of Components I and II are generally higher than Component III. It can be inferred that since Components I and II are terrestrial humic-like fluorophores, and the study sites are mostly agricultural sites (on average, the ratio of agricultural area for monitored catchments is 48.61%), the said fluorophores are dominant in terrestrial and agricultural environments. This inference is in agreement with results from previous studies. In the study of the Horsens Estuary, Denmark, the average FDOM was highest in forest streams and lowest in marine end member. It was also found that the forest stream was dominated by humic-like fluorophores [23]. In another study of the Florida Coastal Everglades, the spatial variation of CDOM in three sub regions (Florida Bay (FB), Ten Thousand Islands (TTI), and Whitewater Bay (WWB)) was investigated. The mean fluorescence intensity of CDOM was higher in TTI and WWB than FB; and the DOM in TTI and WWB was reported to be from a terrestrial source [25].

From Fig. 2, the concentration of Component I is higher than the concentration of Component II throughout the study period. Only the three events mentioned above show that the concentration of Component-III is higher than for Components I and II. Except for the three events, the concentration of Component-III remains below 0.5 throughout the study period. These three events might be the result of activities that are currently unknown to us, and thus require further investigation.

Based on observation, Site 4 appears as the major contributor of Components I and II in the spatial distribution plots (Fig. 2). In most of the events (2008/03, 2008/05, 2008/06, 2008/09, 2008/11, and 2009/01), the concentrations of these two components are one order of magnitude higher compared to the other sites. In the majority of events (2008/08, 2009/02, 2009/04, 2009/07, 2009/08, 2009/10, and 2009/11), the concentrations of the two components at Site 4 are comparable to the other sites. The concentrations of these two humic-like components are unavailable for two events: April and December 2008. In contrast, during the event of June 2009, the concentration of Component I at site 4 is one order of magnitude lower than at Sites 1, 2, 3, and 8. During the same event, the concentration of Component II at Site 4 is one order of magnitude lower than at site 1. From this comparison of Site 4 with the remaining sites, we see that in majority of events Site 4 has a comparable contribution of the two humic-like components. In most of the events, its contribution is one order of magnitude higher than the remaining sties. From these results, we posit that Site 4 is the major contributor of Components I and II. In

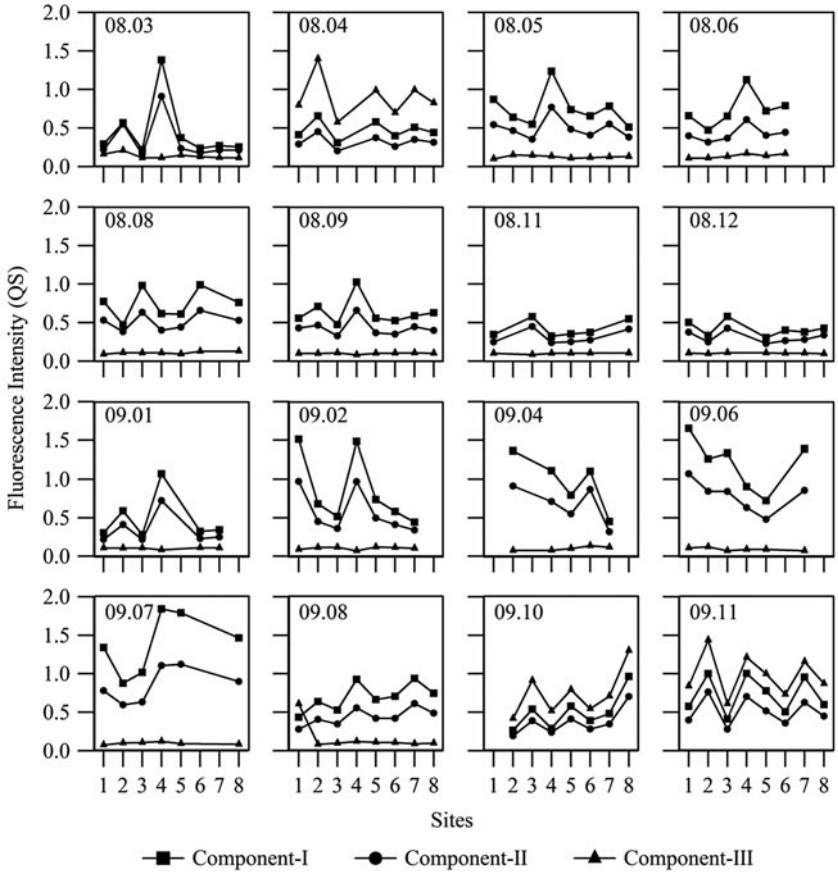


Fig. 2. Spatial variation of PARAFAC components during the study period. Horizontal and vertical axes represent the sampling sites (Site 1 through 8) and fluorescence intensity (QS) respectively. The following nomenclature: YY.MM was used to write the sampling date (e.g. 08.03 is March 2008). Solid lines with square, circular, and triangular markers represent the fluorescence intensities (QS) of Components I, II, and III, respectively.

our study, Site 4 is the largest agricultural area and as such its contribution as the major source of Components I and II becomes more clear. Indeed, this result is in agreement with the studies of Stedmon and Markager [23] and Maie et al. [25].

### 3.3. Temporal variation of FDOM fluorophores

To study the seasonal variation of FDOM fluorophores, the concentrations of identified PARAFAC components were plotted against time for each site. Fig. 3 shows the temporal variation of FDOM fluorophores. Components I and II clearly show similar trends throughout the study period at each site. South Korea has four distinct seasons of snowfall (December to February), spring (March to May), rainfall (June to August), and fall (September to November). The rainfall season in South Korea is considered the monsoon season, characterized by higher precipitation than other seasons. Except for Site 4, the concentrations of Components I and II in spring and summer are higher than in other seasons. These high concentrations can be attributed to snow melting and monsoon rainfall respectively. Also, the concentrations of Components I and II in the rainfall season are higher compared to the remaining three seasons. Heavy rainfall during the monsoon is responsible for the high concentrations of Components I and II in the summer season.

The concentrations of Components I and II in the spring and summer seasons are higher in 2009 than in 2008. The average precipitation in 2008 was recorded to be 173.02 mm, whereas, it was 330.26 mm in 2009. This almost double precipitation in 2009 was a major cause of the high concentrations of Components I and II. An increase in the concentration of humic-like components in FDOM during the wet season has also been observed by other researchers [23,25–27].

Component III shows no seasonal variation at any site. Except for Site 4, the concentration of Component III is notably higher in April 2008 and October and November 2009. Aside from these three months, the concentration of Component III is less than 0.5

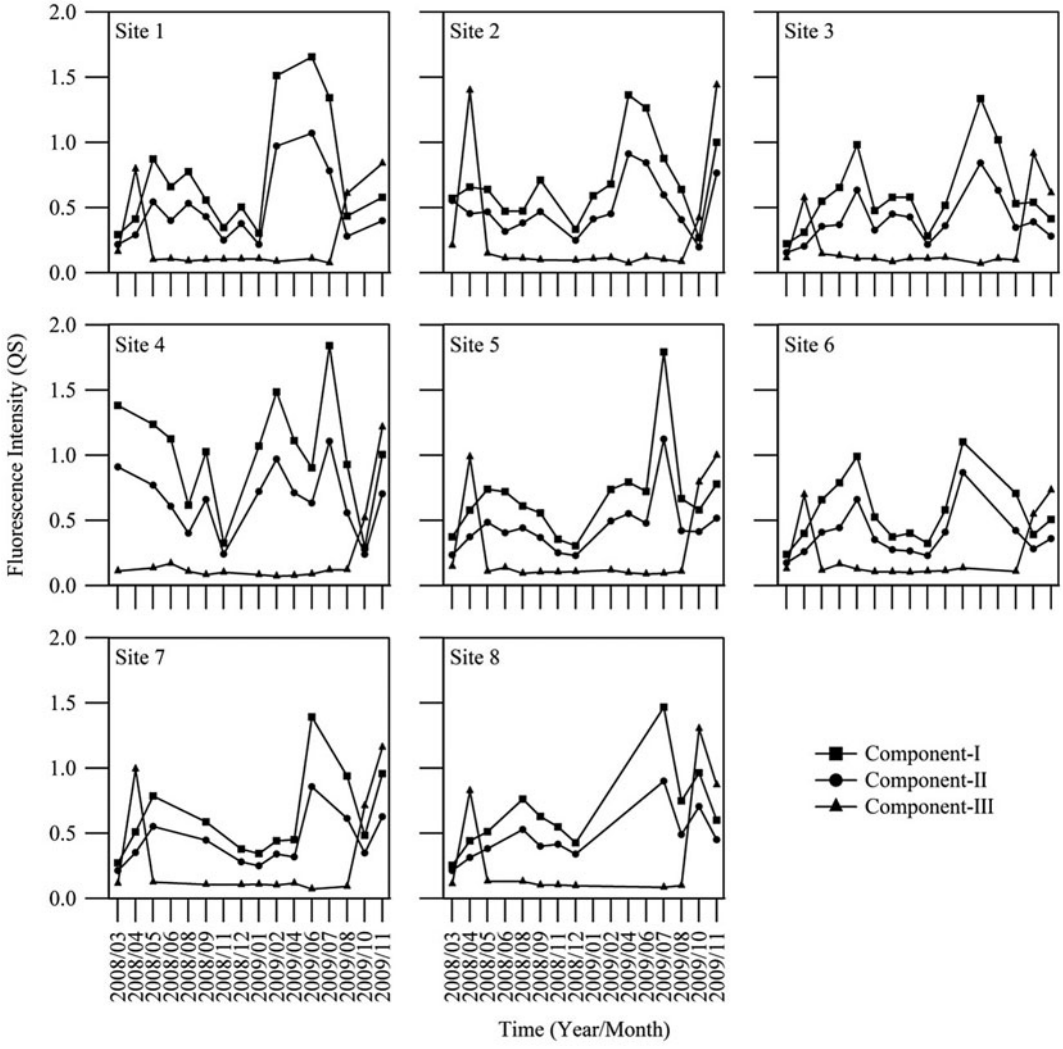


Fig. 3. Temporal variations of PARAFAC components for the eight sites. Horizontal and vertical axes represent the time (Year/Month) and fluorescence intensity (QS), respectively. Solid lines with square, circular, and triangular markers denote the fluorescence intensities (QS) of Components I, II, and III.

throughout the study period on all the sites. This finding is consistent with the study of interannual variation of FDOM in the South Atlantic Bight, where no temporal variation was observed for the marine humic-like component [28]. Based on this result and its agreement with previous studies, we conclude that the marine humic-like component is a constant part of the DOM pool. We therefore suggest that Component III might have some variation in marine environments.

### 3.4. Spatiotemporal variation of FDOM fluorophores

To determine the spatiotemporal variation of FDOM fluorophores, spatiotemporal bubble plots were used (Fig. 4). The bubble plot simultaneously displays spatial and temporal variation. A color gradient is used as a visual aid for ease in viewing the trends. The plot is divided into three panels: the top, middle, and bottom panels representing Components I, II, and III, respectively. The horizontal and vertical axes of each panel represent the time (Year/Month) and sites. Each panel is divided into two parts by a dotted line. The left and right sides of the dotted line represent the FDOM fluorophore concentrations in 2008 and 2009, respectively.

The top two panels of Fig. 4 indicate that Site 4 is the major contributor of Components I and II. In the figure, it is clear that the concentrations of FDOM fluorophores increase during the snow melting and rainfall seasons, suggesting that during these events,

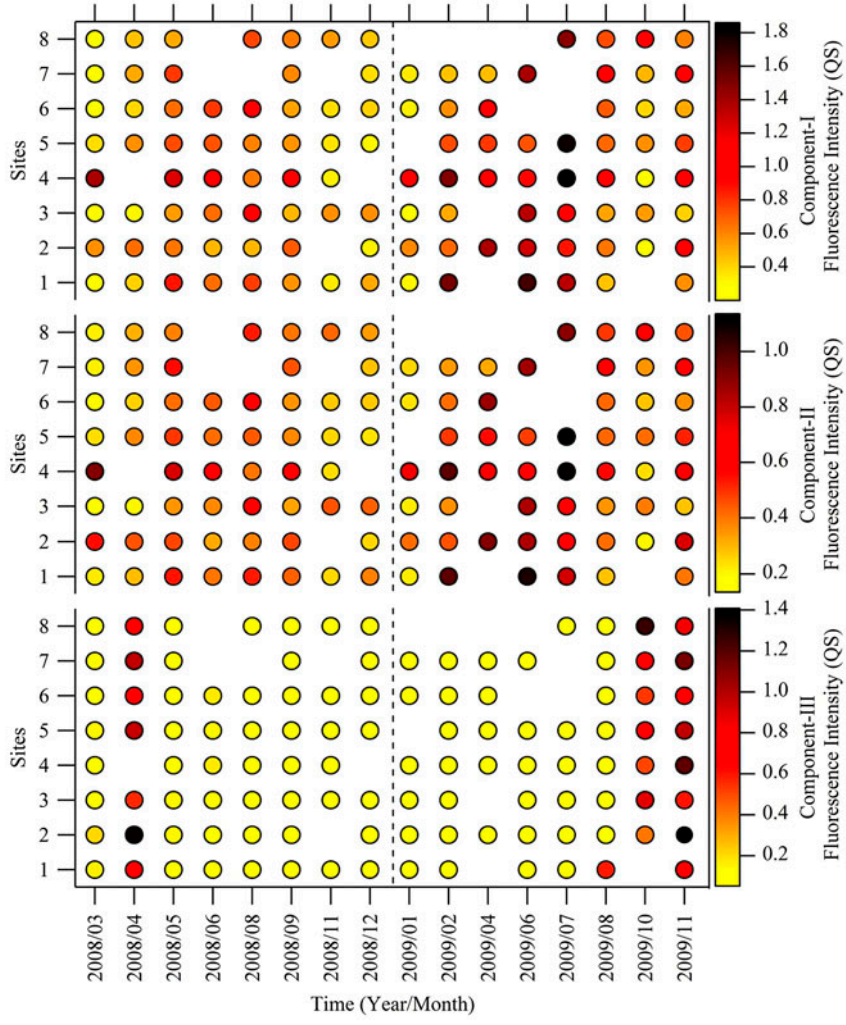


Fig. 4. Spatiotemporal bubble plot of identified PARAFAC components. Horizontal and vertical axes represent the time (Year/Month) and sites, respectively. The bubble colors represent fluorescence intensity (QS) that can be read from the color bar at right side of the plot. The top, middle, and bottom panels of the plot represent the spatiotemporal intensities of PARAFAC Components I, II, and III, respectively. Each panel is divided into halves by a dotted line; the left and right panels represent the fluorescence intensities (QS) in 2008 and 2009.

humus is extracted from the soil and then transferred to into the YSW system through runoff. In addition, the concentrations of Components I and II which were higher in 2009 compared to 2008, can be explained by heavier rainfall that occurred in 2009. The variation of Components I and II with rainfall can be seen in Fig. 5. Panels I, II, III, and IV consist of the average (solid black lines), upper standard deviation (solid red lines), and lower standard deviation (solid blue lines) values for rainfall and the concentrations of the three PARAFAC components. In the figure, Panels II and III (Components I and II) display trends similar to that of Panel I (Rainfall). This indicates that both components originate from the same source and are correlated with rainfall.

The bottom panel of Fig. 5 shows that all eight sites contribute Component III equally to the YSW system. All concentrations are less than 0.2 with the exception of three events: April 2008 and October and November 2009, where there were observed increases in the concentration of Component III. Component III is a mandatory part of marine systems, though it can also be found in riverine systems [22–24]. As such, this marine-like component needs separate attention in riverine systems. Lastly, note also that Component-III has no relation with rainfall (Fig. 5).

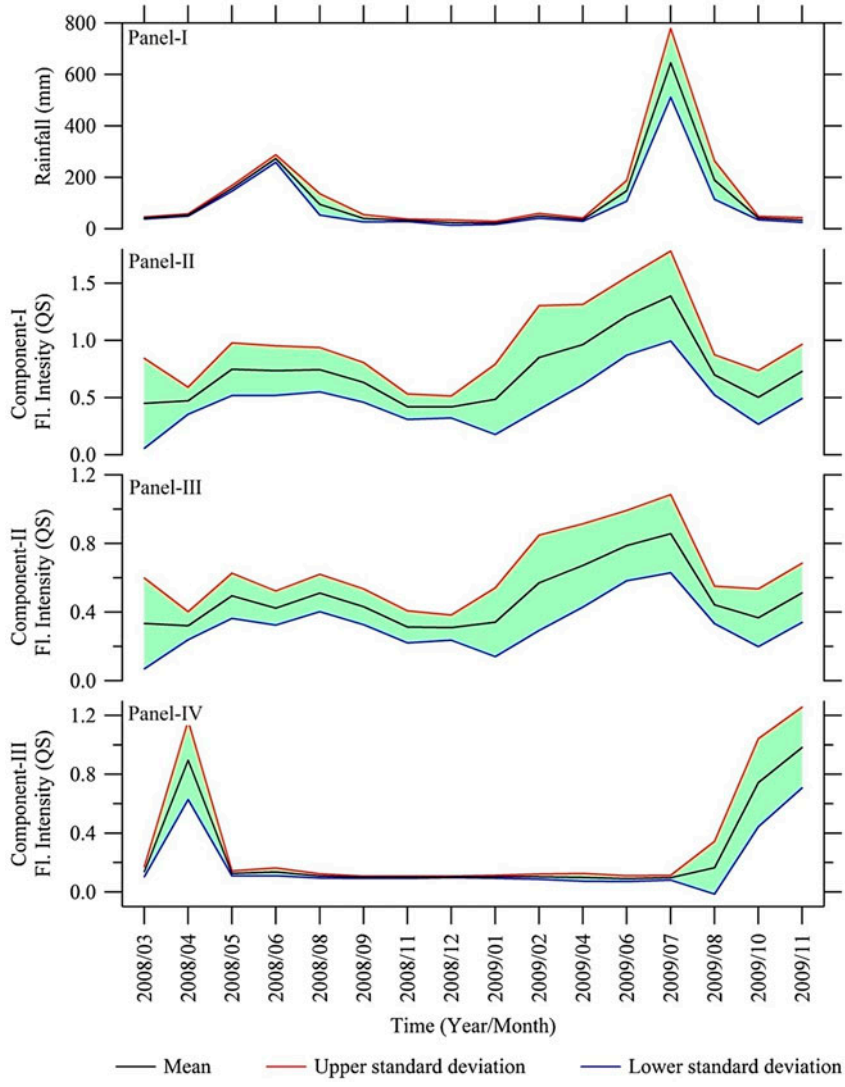


Fig. 5. Correlation of PARAFAC Components I and II with rainfall data. The horizontal axis represents the time (Year/Month) for all four panels of the plot. Vertical axes of Panel II through Panel IV represent the fluorescence intensity (QS), while Panel I represents the rainfall (mm). Note that fluorescence intensities of Components I and II (in Panels II and III, respectively) and rainfall (mm) in Panel I display similar patterns, showing correlation. Black, red, and blue solid lines represent the mean, upper, and lower standard deviations, respectively.

### *3.5. Effect of season and site on identified FDOM fluorophores*

To investigate the effect of season, site, and their combined effect on identified FDOM fluorophores, two-way ANOVA was used. *Post hoc* analysis was also carried out to identify significantly different sites and seasons. A significance level of 0.05 was set for both statistical analyses. Table 2A shows the *F*-test statistics and *p*-values while Table 2B displays the results from the *post hoc* analysis. The upper right diagonal on each panel consists of *p*-values from the *post hoc* analysis of sites, while the bottom left diagonal consists of *p*-values for the seasons.

From Table 2A, it can be seen that the site and season have an effect on Components I and II ($F = 3.16$ and 8.13 for site and season, respectively, and $p < 0.05$). It is also clear that no combined effect of site and season on Component I was be observed ($F = 0.97$ and $p > 0.05$). Similarly, the site and season affect Component II ($F = 2.97$ and 5.31 for site and season, respectively, and $p < 0.05$), though the combined interaction of site and season again does not have a significant effect on Component II ($F = 0.99$ and $p > 0.05$). The YSW is surrounded by sites with varying characteristics and the monsoon season in Korea is deemed to be responsible for this effect.

Table 2A
Effect of season, site, and their interaction on identified FDOM fluorophores

| Dependent variable | Independent variable | *F* | *p*-value |
|---|---|---|---|
| Component I | | | |
| | Site | 3.16 | 0.01 |
| | Season | 8.13 | 0.00 |
| | Site and season | 0.97 | 0.51 |
| Component II | | | |
| | Site | 2.97 | 0.01 |
| | Season | 5.31 | 0.00 |
| | Site and season | 0.99 | 0.48 |
| Component III | | | |
| | Site | 0.22 | 0.98 |
| | Season | 8.18 | 0.00 |
| | Site and season | 0.18 | 1.00 |

The *post hoc* analysis for Component I shows that Site 4 is significantly different from Sites 3, 6, and 7 ($p < 0.05$). The summer season is found to be different from all other seasons ($p < 0.05$). As for the Component II, again Site 4 is significantly different from Sites 3 and 6 ($p < 0.05$). The summer season with monsoon rainfall is again different from other seasons ($p < 0.05$). In the YSW system, Site 4 is the largest agricultural area. Site 2 is the Gwangju tributary, whereas Gwangju city is located near Site 3 (compared to Site 2). Gwangju, being a highly urbanized area, has a high volume of sewer flow in the direction of Site 3. This could be the cause of why Site 3 is significantly different from Site 4. Site 6 on the other hand, is surrounded by mountains, and this site receives runoff from the mountains in the monsoon season, the reason for its significant difference compared to Site 4. As for Site 7, dilution effect caused by its location near

Table 2B
*p*-values for the comparison of sites (upper right shaded diagonal) and seasons (bottom left diagonal) from *post hoc* analysis in two-way ANOVA

| *(a) Component I* | | | | | | | | |
|---|---|---|---|---|---|---|---|---|
| | Site 2 | Site 3 | Site 4 | Site 5 | Site 6 | Site 7 | Site 8 | |
| | 1.00 | 1.00 | 0.48 | 1.00 | 1.00 | 1.00 | 1.00 | Site 1 |
| Winter | 1.00 | 1.00 | 0.23 | 1.00 | 1.00 | 1.00 | 1.00 | Site 2 |
| | | | 0.02 | 1.00 | 1.00 | 1.00 | 1.00 | Site 3 |
| Spring | 1.00 | 1.00 | | 0.16 | 0.01 | 0.06 | 0.19 | Site 4 |
| | | | | | 1.00 | 1.00 | 1.00 | Site 5 |
| Summer | 0.00 | 0.00 | 0.00 | | | 1.00 | 1.00 | Site 6 |
| | | | | | | | 1.00 | Site 7 |
| | Fall | Winter | Spring | | | | | |
| *(b) Component II* | | | | | | | | |
| | Site 2 | Site 3 | Site 4 | Site 5 | Site 6 | Site 7 | Site 8 | |
| | 1.00 | 1.00 | 0.68 | 1.00 | 1.00 | 1.00 | 1.00 | Site 1 |
| Winter | 1.00 | 1.00 | 1.00 | 1.00 | 1.00 | 1.00 | 1.00 | Site 2 |
| | | | 0.03 | 1.00 | 1.00 | 1.00 | 1.00 | Site 3 |
| Spring | 1.00 | 1.00 | | 0.21 | 0.02 | 0.17 | 0.59 | Site 4 |
| | | | | | 1.00 | 1.00 | 1.00 | Site 5 |
| Summer | 0.01 | 0.01 | 0.03 | | | 1.00 | 1.00 | Site 6 |
| | | | | | | | 1.00 | Site 7 |
| | Fall | Winter | Spring | | | | | |
| *(c) Component III* | | | | | | | | |
| | Site 2 | Site 3 | Site 4 | Site 5 | Site 6 | Site 7 | Site 8 | |
| | 1.00 | 1.00 | 1.00 | 1.00 | 1.00 | 1.00 | 1.00 | Site 1 |
| Winter | 0.00 | 1.00 | 1.00 | 1.00 | 1.00 | 1.00 | 1.00 | Site 2 |
| | | | 1.00 | 1.00 | 1.00 | 1.00 | 1.00 | Site 3 |
| Spring | 0.27 | 0.20 | | 1.00 | 1.00 | 1.00 | 1.00 | Site 4 |
| | | | | | 1.00 | 1.00 | 1.00 | Site 5 |
| Summer | 0.00 | 1.00 | 0.16 | | | 1.00 | 1.00 | Site 6 |
| | | | | | | | 1.00 | Site 7 |
| | Fall | Winter | Spring | | | | | |

downstream of the YSR brings about the difference. In the Midwestern Bay of Bengal, humic C has been reported to be affected by the wet season, during which the concentration of humic C is reported [28,29]. Evidences of high concentration of humic C in terrestrial and forest streams have already been published [23,28].

Component III (see Table 2A) is not significantly affected by site ($F = 0.22$, $p > 0.05$), though it is affected by season ($F = 8.18$, $p < 0.05$). The site and season in combination have no effect on Component III ($F = 0.18$, $p > 0.05$). *Post hoc* analysis also shows that the fall season is significantly different from winter and summer (Table 2B). Since Component III is a marine humic component, its behavior can be understood better from a marine environment. Unlike our results, no interannual variation of marine humic M was observed in the South Atlantic Bight [28]. This difference is due to the fact that spatiotemporal plots present only a visualization analysis where the results can be misleading. We posit that the ANOVA used here has provided information that might be more reliable.

## 4. Conclusion

This study provides a detailed discussion on FDOM fluorophore characterization and spatiotemporal variation at the eight sampling sites surrounding the YSR; which is then followed by investigation of the sources and sinks of the identified FDOM fluorophores. The main conclusions of the study are given below.

(1) Three PARAFAC components were identified through PARAFAC modeling of spectrophotometric EEM data. These three components, labeled as Components I, II, and III, were characterized by humic C3 (355/450), humic C (320/405), and marine humic M (280/410) like fluorescence, respectively. The PARAFAC model used in this study explained 95.32% of the variation in data, indicating that it is robust and suitable for three-way data (like spectrophotometric EEM data). PARAFAC is more powerful than two way principal component analysis (PCA), Tucker model, etc. when it comes to the analysis of EEMs. Therefore, we suggest the use of PARAFAC model for the characterization of FDOM fluorophores in three-way spectrophotometric EEM data.

(2) Of the eight sampling sites, Site 4 was the biggest agricultural area around the YSW. Higher concentrations of Components I and II were found at this site, suggesting that agricultural soil could be the main source of these components. Of the four seasons, higher concentration of Components I and II were found in the summer and spring seasons, indicating that rainfall and snow melting events bring FDOMs into the YSW mainstream. Based on these findings, we suggest that best management practices be considered during rainfall and snow melting event to mitigate river impaction by FDOM fluorophores. Note that a spatiotemporal analysis of Component III showed that it remained invariant.

(3) The analysis of FDOM fluorophore concentration data by ANOVA showed that Components I and II were affected by site and season ($p < 0.05$). We also found that Component III was affected by season only ($p < 0.05$). The analysis of FDOM fluorophore concentration data by ANOVA provided a new information about Component III—it is affected by season. From these results, we recommend the further use of ANOVA and similar higher order statistical models during investigations of FDOM fluorophore concentration data.

(4) *Post hoc* analysis revealed that Site 4 was significantly different from Sites 3 and 6 for Components I and II ($p < 0.05$). We also found that the summer season was significantly different from all other seasons ($p < 0.05$) for Components I and II, and that the fall season was significantly different from winter and summer seasons for Component III ($p < 0.05$). These findings of significantly different sites and seasons could be a new contribution to this research field and thus further investigation of different environments is needed. We therefore recommend the use of *post hoc* analysis on other FDOM fluorophore concentration data to determine significantly different sites and seasons.

## Supplementary material

The supplementary material for this paper is available online at http://dx.doi.10.1080/19443994.2015.1112978.

## Acknowledgement

This research was supported by the Basic Science Research Program through the National Research Foundation of Korea (NRF) funded by the Ministry of Education, Science and Technology (2010-0011822), Korea.

## References


[1] J.H. Kang, S.W. Lee, K.H. Cho, S.J. Ki, S.M. Cha, J.H. Kim, Linking land-use type and stream water quality using spatial data of fecal indicator bacteria and heavy metals in the Yeongsan river basin, Water Res. 44 (2010) 4143–4157.

[2] S.J. Ki, J.-H. Kang, S.W. Lee, Y.S. Lee, K.H. Cho, K.-G. An, J.H. Kim, Advancing assessment and design of stormwater monitoring programs using a self-organizing map: Characterization of trace metal concentration profiles in stormwater runoff, Water Res. 45 (2011) 4183–4197.

[3] Y.G. Lee, K.G. An, P.T. Ha, K.Y. Lee, J.H. Kang, S.M. Cha, K.H. Cho, Y.S. Lee, I.S. Chang, K.-W. Kim, J.H. Kim, Decadal and seasonal scale changes of an artificial lake environment after blocking tidal flows in the Yeongsan Estuary region, Korea, Sci. Total Environ. 407 (2009) 6063–6072.

[4] A. Baker, Fluorescence excitation−emission matrix characterization of some sewage-impacted rivers, Environ. Sci. Technol. 35 (2001) 948–953.

[5] K.M.G. Mostofa, T. Yoshioka, E. Konohira, E. Tanoue, Photodegradation of fluorescent dissolved organic matter in river waters, Geochem. J. 41 (2007) 323–331.

[6] B. Nieke, R. Reuter, R. Heuermann, H. Wang, M. Babin, J.C. Therriault, Light absorption and fluorescence properties of chromophoric dissolved organic matter (CDOM), in the St. Lawrence Estuary (Case 2 waters), Cont. Shelf Res. 17 (1997) 235–252.

[7] E.M. Carstea, A. Baker, M. Bieroza, D. Reynolds, Continuous fluorescence excitation–emission matrix monitoring of river organic matter, Water Res. 44 (2010) 5356–5366.

[8] C.A. Stedmon, B. Seredyńska-Sobecka, R. Boe-Hansen, N. Le Tallec, C.K. Waul, E. Arvin, A potential approach for monitoring drinking water quality from groundwater systems using organic matter fluorescence as an early warning for contamination events, Water Res. 45 (2011) 6030–6038.

[9] C.M. Andersen, R. Bro, Practical aspects of PARAFAC modeling of fluorescence excitation-emission data, J. Chemom. 17 (2003) 200–215.

[10] J. Christensen, E.M. Becker, C.S. Frederiksen, Fluorescence spectroscopy and PARAFAC in the analysis of yogurt, Chemom. Intell. Lab. Syst. 75 (2005) 201–208.

[11] S. Comero, G. Locoro, G. Free, S. Vaccaro, L. De Capitani, B.M. Gawlik, Characterisation of Alpine lake sediments using multivariate statistical techniques, Chemom. Intell. Lab. Syst. 107 (2011) 24–30.

[12] X. Luciani, S. Mounier, H.H.M. Paraquetti, R. Redon, Y. Lucas, A. Bois, L.D. Lacerda, M. Raynaud, M. Ripert, Tracing of dissolved organic matter from the SEPETIBA Bay (Brazil) by PARAFAC analysis of total luminescence matrices, Mar. Environ. Res. 65 (2008) 148–157.

[13] L.G. Thygesen, Å. Rinnan, S. Barsberg, J.K.S. Møller, Stabilizing the PARAFAC decomposition of fluorescence spectra by insertion of zeros outside the data area, Chemom. Intell. Lab. Syst. 71 (2004) 97–106.

[14] C.A. Stedmon, R. Bro, Characterizing dissolved organic matter fluorescence with parallel factor analysis: A tutorial, Limnol. Oceanogr. Methods 6 (2008) 572–579.

[15] P.G. Coble, Characterization of marine and terrestrial DOM in seawater using excitation-emission matrix spectroscopy, Mar. Chem. 51 (1996) 325–346.

[16] J.B. Fellman, R.G.M. Spencer, P.J. Hernes, R.T. Edwards, D.V. D'Amore, E. Hood, The impact of glacier runoff on the biodegradability and biochemical composition of terrigenous dissolved organic matter in near-shore marine ecosystems, Mar. Chem. 121 (2010) 112–122.

[17] C. Guéguen, M.A. Granskog, G. McCullough, D.G. Barber, Characterisation of colored dissolved organic matter in Hudson Bay and Hudson Strait using parallel factor analysis, J. Mar. Syst. 88 (2011) 423–433.

[18] N. Hudson, A. Baker, D. Reynolds, Fluorescence analysis of dissolved organic matter in natural, waste and polluted waters—A review, River Res. Appl. 23 (2007) 631–649.

[19] K.R. Murphy, C.A. Stedmon, T.D. Waite, G.M. Ruiz, Distinguishing between terrestrial and autochthonous organic matter sources in marine environments using fluorescence spectroscopy, Mar. Chem. 108 (2008) 40–58.

[20] C.A. Stedmon, S. Markager, R. Bro, Tracing dissolved organic matter in aquatic environments using a new approach to fluorescence spectroscopy, Mar. Chem. 82 (2003) 239–254.

[21] Y. Zhang, M.A. van Dijk, M. Liu, G. Zhu, B. Qin, The contribution of phytoplankton degradation to chromophoric dissolved organic matter (CDOM) in eutrophic shallow lakes: Field and experimental evidence, Water Res. 43 (2009) 4685–4697.

[22] P.G. Coble, Marine optical biogeochemistry: The chemistry of ocean color, Chem. Rev. 107 (2007) 402–418.

[23] C.A. Stedmon, S. Markager, Resolving the variability in dissolved organic matter fluorescence in a temperate estuary and its catchment using PARAFAC analysis, Limnol. Oceanogr. 50 (2005) 686–697.

[24] L. Jørgensen, C.A. Stedmon, T. Kragh, S. Markager, M. Middelboe, M. Søndergaard, Global trends in the fluorescence characteristics and distribution of marine dissolved organic matter, Mar. Chem. 126 (2011) 139–148.

[25] N. Maie, J.N. Boyer, C. Yang, R. Jaffé, Spatial, geomorphological, and seasonal variability of CDOM in estuaries of the Florida Coastal Everglades, Hydrobiologia 569 (2006) 135–150.

[26] R. Jaffé, J.N. Boyer, X. Lu, N. Maie, C. Yang, N.M. Scully, S. Mock, Source characterization of dissolved organic matter in a subtropical mangrove-dominated estuary by fluorescence analysis, Mar. Chem. 84 (2004) 195–210.

[27] Y. Zhang, Y. Yin, L. Feng, G. Zhu, Z. Shi, X. Liu, Y. Zhang, Characterizing chromophoric dissolved organic matter in Lake Tianmuhu and its catchment basin using excitation-emission matrix fluorescence and parallel factor analysis, Water Res. 45 (2011) 5110–5122.

[28] P. Kowalczuk, M.J. Durako, H. Young, A.E. Kahn, W.J. Cooper, M. Gonsior, Characterization of dissolved organic matter fluorescence in the South Atlantic Bight with use of PARAFAC model: Interannual variability, Mar. Chem. 113 (2009) 182–196.

[29] N.V.H.K. Chari, N.S. Sarma, S.R. Pandi, K.N. Murthy, Seasonal and spatial constraints of fluorophores in the midwestern Bay of Bengal by PARAFAC analysis of excitation emission matrix spectra, Estuarine Coastal Shelf Sci. 100 (2012) 162–171.